THE ASTROPHYSICAL JOURNAL, 500:14–27, 1998 June 10

THE COSMOLOGICAL MASS DISTRIBUTION FUNCTION IN THE ZELDOVICH APPROXIMATION

JOUNGHUN LEE AND SERGEI F. SHANDARIN
Department of Physics and Astronomy, University of Kansas, Lawrence, KS 66045; taiji@kusmos.phsx.ukans.edu, sergei@kusmos.phsx.ukans.edu
Received 1997 July 23; accepted 1998 January 22

ABSTRACT

An analytic approximation of the mass function for gravitationally bound objects is presented. Based on the Zeldovich approximation, we extend the Press-Schechter formalism to a nonspherical dynamical model. A simple extrapolation of that approximation suggests that the gravitational collapse along all three directions, which eventually leads to the formation of real virialized object clumps, occurs in the regions where the lowest eigenvalue of the deformation tensor, λ_3, is positive. We derive the conditional probability of $\lambda_3 > 0$ as a function of the linearly extrapolated density contrast δ and the conditional probability distribution of δ, provided that $\lambda_3 > 0$. These two conditional probability distributions show that the most probable density of the bound regions ($\lambda_3 > 0$) is roughly 1.5 on the characteristic mass scale M_* and that the probability of $\lambda_3 > 0$ is almost unity in the highly overdense regions ($\delta > 3\sigma$). Finally, an analytic mass function of clumps is derived with the help of one simple *Ansatz*, which is employed to treat the multistream regime beyond the validity of the Zeldovich approximation. The resulting mass function is renormalized by a factor of 12.5, which we justify with a sharp k-space filter by means of the modified Jedamzik analysis. Our mass function is shown to be different from the Press-Schechter one, having a lower peak and predicting more small-mass objects.

Subject headings: cosmology: theory — galaxies: clusters: general — large-scale structure of universe

1. INTRODUCTION

Our present universe is observed to be quite clumpy, with numerous galaxies, groups of galaxies, galaxy clusters, etc., which span a large dynamic range in mass. The mass distribution function of these large-scale structures is a crucial key to the nature of primordial density fluctuations from which the cosmic structures are believed to have arisen through gravitational growth, recollapse, and virialization (Kolb & Turner 1990). Since these gravitational processes are inherently nonlinear and sufficiently complicated, it is not an easy task to find analytically the mass distribution function for bound objects. Owing to its important role in cosmology, however, much effort has been made to determine even an approximate expression of the mass function (e.g., Peebles 1985; Williams et al. 1991; Brainerd & Villumsen 1992; Cavaliere & Menci 1994; Vergassola et al. 1994; Cavaliere, Menci, & Tozzi 1996). For a recent review, see Monaco (1997).

The pioneering attempt in this field has been ascribed to Press & Schechter (1974, hereafter PS),[1] who proposed an analytic formalism for the mass function based on two simple assumptions: (1) the initial density field is Gaussian, and (2) the gravitational collapse of mass elements is spherical and homogeneous. Along with these two assumptions, PS also postulated that the number densities of bound objects could be counted by filtering the initial linear density field. Although much criticism thereafter was poured on the PS formalism regarding its unrealistic treatment of the collapse process and unclarified arguments, including the *notorious* normalization factor of 2, the PS mass function has survived many numerical tests, showing good agreement with the results from N-body simulations (e.g., Efstathiou et al. 1988; Bond et al. 1991; Lacey & Cole 1994).

Motivated by the somewhat unexpected success of the PS mass function, many authors have tried to understand why it works so well in practice. Peacock & Heavens (1990) and Bond et al. (1991) have shown, by using the excursion set theory, that the "fudge factor" of 2 in the PS formalism, which is directly related to the cloud-in-cloud problem, can be justified with a sharp k-space filter. Jedamzik (1995) solved this cloud-in-cloud problem by means of the integral equation for the mass function. He insisted that the PS mass function should be altered even in the case of a sharp k-space filter. Yet Yano, Nagashima, & Gouda (1996) have argued that the sharp k-space filter recovers the PS mass function with the normalization factor of 2 even in the Jedamzik formalism if a mathematically consistent definition of isolated bound objects is used and the spatial correlations are neglected. They have also shown by introducing the two-point correlation function into the Jedamzik formalism that the possible overlapping effect of density fluctuations, which is responsible for the fragmentation and the coagulation of bound objects (see Silk & White 1978; Lucchin 1988; Cavaliere & Menci 1993), can be neglected either on very small or on large mass scales.

The PS approach has been also applied to nonspherical dynamical models. Monaco (1995) has suggested that the mass function should be treated as a Lagrangian quantity. Employing the Zeldovich approximation as a proper Lagrangian dynamics, he computed the collapse epoch along the first principal axis and showed that the shear shortens the collapse time and thus that more high-mass structures are expected to form than the original PS mass function predicts. This effect of the shear explains dynamically the lowered density threshold ($\delta_c \simeq 1.5$) detected in several N-body experiments (e.g., Efstathiou & Rees 1988; Carlberg & Couchman 1989; Klypin et al. 1995; Bond & Myers 1996).

Shandarin & Klypin (1984) have shown by N-body simulations that nonlinear clumps form from the Lagrangian regions where the smallest eigenvalue of the deformation tensor, λ_3, reaches a local maximum. Recently, Audit, Teyssier, & Alimi

[1] See also Doroshkevich (1967).

(1997) have proposed some analytic prescriptions to compute the collapse time along the second and the third principal axes, pointing out that Lagrangian dynamics is not valid after the first-axis collapse but that the formation of real virialized clumps must correspond to the third-axis collapse. Their argument agrees with the N-body result obtained by Shandarin & Klypin (1984). In their analysis, the shear delays the third-axis collapse rather than fastens it, in contrast to its effect on the first-axis collapse, which is in agreement with Peebles (1990).

The normalization problem, however, has not been well addressed in these nonspherical approaches to the mass function. Monaco (1995) adopted the normalization factor of 2 used in the PS formalism, while Audit et al. (1997) just assumed that the mass function could be normalized properly in any case.

In this paper we study the eventual formation of clumps in a spatially flat matter-dominated universe, with fragmentation and coagulation effects ignored. In § 2, we review the statistical treatment of the mass function, highlighting the PS formalism. In § 3, a nonspherical approach to the collapse condition based on the Zeldovich approximation is described, and two useful conditional probability distributions relating the density field to the collapse condition are derived. In § 4, an *Ansatz* is proposed to extend the validity of the Lagrangian dynamics to the third-axis collapse. With a help of this *Ansatz*, an analytic approximation to the mass function for clumps is derived. In § 5, we justify the normalization factor 12.5 of the resulting mass function by using the Jedamzik integral equation. In § 6, the results are discussed and final conclusions are drawn. We relegate the detailed calculations and derivations to Appendices A and B.

2. STATISTICAL DESCRIPTION OF MASS FUNCTIONS

The mass function $n(M)$ is defined such that $n(M)dM$ is the comoving number density of gravitationally bound objects in the mass range $(M, M + dM)$. To compute this statistic, it is assumed that the number densities of bound objects can be inferred from the linearly extrapolated density contrast field, $\delta \equiv \delta\rho/\bar{\rho}$ (where $\bar{\rho}$ is the mean density). In other words, if a given region of the linear density field satisfies a specified criterion of collapse, then it is supposed to collapse and form a bound object.

Let $F(M)$ be the probability of finding a region satisfying a given collapse condition in the linear density field filtered at mass scale M or, equivalently, the fraction of the volume occupied by the regions that will eventually collapse into bound objects with masses greater than M. Then we may write $F(M)$ as follows:

$$F(M) = \int_{-1}^{\infty} p(\delta) C \, d\delta \, . \tag{1}$$

Here $p(\delta)d\delta$ is the probability that the smoothed density field at any given point will have a value in the range $(\delta, \delta + d\delta)$ and C stands for the probability that the chosen point with density δ will actually collapse. Once $p(\delta)$ and C are determined and $F(M)$ is found, the mass function $n(M)$ can be easily obtained as

$$n(M) = \frac{\bar{\rho}}{M} \left| \frac{dF}{dM} \right| , \tag{2}$$

where $M/\bar{\rho}$ is nothing but the volume of a bound region with mass M.

The specific functional form of C is determined by the chosen dynamics to explain the collapse process, while $p(\delta)$ depends on the property of the initial density field, which is often assumed to be Gaussian in the standard cosmology (see Bardeen et al. 1986). The probability distribution of the Gaussian density field smoothed out by a window function $W(R)$ of scale radius R is given by

$$p(\delta) = \frac{1}{\sqrt{2\pi}\sigma(M)} \exp\left[-\frac{\delta^2}{2\sigma^2(M)}\right] . \tag{3}$$

Here the mass variance $\sigma^2(M)$ is a function of scale mass $M \propto \bar{\rho} R^3$ and is estimated by

$$\sigma^2(M) = \int \frac{d^3k}{(2\pi)^3} |\delta_k|^2 W_k^2(R) \, , \tag{4}$$

where δ_k and $W_k(R)$ are the Fourier components of the density δ and the window function $W(R)$, respectively.

According to the top-hat spherical model adopted by PS, the bound objects form in the regions where the linearly extrapolated density contrast δ, growing with time, reaches its critical value $\delta_c \simeq 1.69$ in a flat universe (Peebles 1993). Therefore, the regions with $\delta > \delta_c$, when filtered at scale radius R, correspond to the bound objects with masses greater than $M(R)$, since they will have $\delta = \delta_c$ when filtered at some larger scale. Thus, in the PS formalism, the collapse probability C in equation (1) is determined solely by the density field itself and can be expressed by the following Heaviside step function:

$$C_{\rm PS} = \Theta(\delta - \delta_c) . \tag{5}$$

Using equations (1), (3), and (5), one obtains

$$\begin{aligned} F(M) &= \frac{1}{\sqrt{2\pi}\sigma(M)} \int_{-1}^{\infty} \exp\left[-\frac{\delta^2}{2\sigma^2(M)}\right]\Theta(\delta - \delta_c)d\delta , \\ &= \frac{1}{\sqrt{2\pi}\sigma(M)} \int_{\delta_c}^{\infty} \exp\left[-\frac{\delta^2}{2\sigma^2(M)}\right]d\delta , \\ &= \frac{1}{2}\,{\rm erfc}\left[\frac{\delta_c}{\sqrt{2}\sigma(M)}\right], \end{aligned} \tag{6}$$

where erfc (x) is the complementary error function.

One obvious problem with the above analysis is that the integral of dF/dM over the whole range of mass does not give unity:

$$\int_0^{\infty} \frac{dF}{dM}\,dM = \int_0^{\infty} dF = \frac{1}{2} . \tag{7}$$

This normalization problem originates from the fact that the PS formalism does not properly account for the underdense regions. Even for regions with $\delta < \delta_c$ at a given filtering scale, there is still a *nonzero* probability that such regions will have $\delta > \delta_c$ when filtered at some larger scale. But the PS formalism completely ignored those underdense regions in estimating $F(M)$, so half the mass initially present in the underdense regions was not taken care of. PS avoided this normalization problem simply by multiplying dF/dM by a factor of 2 and wrote the mass function in the form such that

$$\begin{aligned} n_{\rm PS}(M) &= 2\,\frac{\bar{\rho}}{M}\left|\frac{dF}{dM}\right| = 2\,\frac{\bar{\rho}}{M}\left|\frac{d\sigma}{dM}\frac{\partial F}{\partial \sigma}\right| , \\ &= \sqrt{\frac{2}{\pi}}\,\frac{\bar{\rho}}{M}\left|\frac{d\sigma}{dM}\right|\frac{\delta_c}{\sigma^2(M)}\exp\left[-\frac{\delta_c^2}{2\sigma^2(M)}\right]. \end{aligned} \tag{8}$$

As mentioned in § 1, the "cooked-up" normalization factor of 2 in equation (8) has been shown to be correct in the case of a sharp k-space filter $[W_k(R) = \Theta(\pi/R - k)]$, and various numerical tests have confirmed the PS mass function as a satisfactory approximation. Nevertheless, it still leaves much to be desired. The physical meaning of the sharp k-space filter has yet to be understood; the gravitational collapse should be treated in more realistic models than the top-hat spherical one; the lowered density threshold ($\delta_c \simeq 1.5$) obtained in many numerical tests cannot be explained by this statistical argument, so the PS mass function is degraded to a phenomenological device.

3. NONSPHERICAL APPROACH TO THE COLLAPSE CONDITION

Since PS derived their mass function on the basis of the top-hat spherical model in 1974, the nonspherical nature of the gravitational collapse has been demonstrated by many authors (e.g., Shandarin et al. 1995; Kuhlman, Melott, & Shandarin 1996). The shear especially has been shown to play a very important role in the formation of the nonlinear structures (e.g., Peebles 1990; Monaco 1995; Audit et al. 1997). Therefore, it is necessary to consider more realistic dynamical models to understand the collapse process and find the mass function.

We choose the Zeldovich approximation as a suitable Lagrangian dynamics to take into account the nonspherical aspect of the gravitational collapse. However, instead of bringing the effect of the shear up to the surface, we try to retain the framework of the PS formalism, counting the number densities of bound objects from the filtered linear density field but with a different dynamical collapse probability C in equation (1).

3.1. *The Zeldovich Approximation*

The Zeldovich approximation (Zeldovich 1970) asserts that the trajectory of a cosmic particle in the comoving coordinates can be expressed by the following simple formula:

$$\boldsymbol{x} = \boldsymbol{q} - D_+(t)\nabla\Psi(\boldsymbol{q}) . \tag{9}$$

Here $\boldsymbol{q}$ and $\boldsymbol{x}$ are the Lagrangian (initial) and the Eulerian (final) coordinates, respectively, the particle $\Psi(\boldsymbol{q})$ is the perturbation potential, which is a Gaussian random field, and $D_+(t)$ describes the growth of density fluctuations as a function of time. Throughout this paper, we focus on a spatially flat matter-dominated universe with vanishing cosmological constant, in which case $D_+(t) \propto a(t) \propto t^{2/3}$ [where $a(t)$ is the cosmic expansion factor].

Applying a simple mass conservation relation $\bar{\rho}\, d^3\boldsymbol{q} = \rho(x) d^3x$ to equation (9) gives the following expression of the mass density:

$$\rho(x) = \frac{\bar{\rho}}{[1 - D_+(t)\lambda_1(\boldsymbol{q})][1 - D_+(t)\lambda_2(\boldsymbol{q})][1 - D_+(t)\lambda_3(\boldsymbol{q})]}, \tag{10}$$

where $\lambda_1, \lambda_2, \lambda_3$ are the ordered eigenvalues ($\lambda_1 > \lambda_2 > \lambda_3$) of the deformation tensor,

$$d_{ij} = \frac{\partial^2 \Psi}{\partial q_i \partial q_j}. \tag{11}$$

Equation (10) shows that the three random fields $\lambda_1(\boldsymbol{q})$, $\lambda_2(\boldsymbol{q})$, $\lambda_3(\boldsymbol{q})$ in the Lagrangian space are now the new dynamic quantities determining the collapse condition of given cosmic masses in the corresponding Eulerian space. Thus, the mass function of bound objects can be built on this Lagrangian dynamical theory (see also Monaco 1995).

The actual dynamics for the formation of gravitationally bound objects is very complex. Even in the frame of the Zeldovich approximation, the description of the gravitational collapse along all three directions is far from being simple and is too cumbersome to use (Arnold, Shandarin, & Zeldovich 1982). Here we employ rather a simplified dynamical model to approximate the collapse process and determine the collapse condition for the formation of clumps.

Provided that at least one of the eigenvalues is positive at a given (Lagrangian) point, the denominator in equation (10) can become zero as $D_+(t)$ increases with time, so the density $\rho(x)$ will diverge, signaling collapse at the corresponding Eulerian point. If only the largest eigenvalue is positive ($\lambda_1 > 0$, $\lambda_3 < \lambda_2 < 0$) in a given region, then it collapses into a pancake. If two eigenvalues are positive ($\lambda_1 > \lambda_2 > 0$) while the third one is negative ($\lambda_3 < 0$), then a filament forms. The formation of a virialized bound object clump occurs only if all three eigenvalues are positive, i.e., $\lambda_3 > 0$. So, in our dynamical model based on the Zeldovich approximation, it is assumed that the lowest eigenvalue, λ_3, plays the most crucial role in determining the collapse condition for the formation of clumps. This assumption is in general agreement with Shandarin & Klypin (1984).

The useful joint probability distribution of an ordered set (λ_1, λ_2, λ_3) is derived by Doroshkevich (1970):

$$p(\lambda_1, \lambda_2, \lambda_3) = \frac{3375}{8\sqrt{5}\pi\sigma^6} \exp\left(-\frac{3I_1^2}{\sigma^2} + \frac{15I_2}{2\sigma^2}\right)(\lambda_1 - \lambda_2)(\lambda_2 - \lambda_3)(\lambda_1 - \lambda_3), \tag{12}$$

where $I_1 = \lambda_1 + \lambda_2 + \lambda_3$, $I_2 = \lambda_1\lambda_2 + \lambda_2\lambda_3 + \lambda_3\lambda_1$, and σ^2 is the mass variance as defined in equation (4). From equation (12), one can see that the Zeldovich approximation excludes both exactly spherical ($\lambda_1 = \lambda_2 = \lambda_3$) and exactly cylindrical ($\lambda_1 = \lambda_2$, $\lambda_2 = \lambda_3$, $\lambda_3 = \lambda_1$) collapse. Both types of collapse have zero probability of occurring. (However, the points with $\lambda_i = \lambda_j$ exist in generic fields on lines, that is, on a set of measure zero in three dimensions, while the points with $\lambda_1 = \lambda_2 = \lambda_3$ do not exist at all.)

In order to obtain a deeper qualitative understanding of the collapse in the Zeldovich approximation, it may be also useful, in addition to this joint probability distribution equation (12), to have an individual probability distribution of each eigenvalue[2] (see Appendix A):

$$\begin{aligned} p(\lambda_1) = \frac{\sqrt{5}}{12\pi\sigma}\Bigg[& 20\frac{\lambda_1}{\sigma}\exp\left(-\frac{9\lambda_1^2}{2\sigma^2}\right) - \sqrt{2\pi}\exp\left(-\frac{5\lambda_1^2}{2\sigma^2}\right)\operatorname{erf}\left(\sqrt{2}\frac{\lambda_1}{\sigma}\right)\left(1 - 20\frac{\lambda_1^2}{\sigma^2}\right) - \sqrt{2\pi}\exp\left(-\frac{5\lambda_1^2}{2\sigma^2}\right)\left(1 - 20\frac{\lambda_1^2}{\sigma^2}\right) \\ & + 3\sqrt{3\pi}\exp\left(-\frac{15\lambda_1^2}{4\sigma^2}\right)\operatorname{erf}\left(\frac{\sqrt{3}\lambda_1}{2\sigma}\right) + 3\sqrt{3\pi}\exp\left(-\frac{15\lambda_1^2}{4\sigma^2}\right)\Bigg], \end{aligned} \tag{13}$$

$$p(\lambda_2) = \frac{\sqrt{15}}{2\sqrt{\pi}\sigma}\exp\left(-\frac{15\lambda_2^2}{4\sigma^2}\right), \tag{14}$$

$$\begin{aligned} p(\lambda_3) = -\frac{\sqrt{5}}{12\pi\sigma}\Bigg[& 20\frac{\lambda_3}{\sigma}\exp\left(-\frac{9\lambda_3^2}{2\sigma^2}\right) + \sqrt{2\pi}\exp\left(-\frac{5\lambda_3^2}{2\sigma^2}\right)\operatorname{erfc}\left(\sqrt{2}\frac{\lambda_3}{\sigma}\right)\left(1 - 20\frac{\lambda_3^2}{\sigma^2}\right) \\ & - 3\sqrt{3\pi}\exp\left(-\frac{15\lambda_3^2}{4\sigma^2}\right)\operatorname{erfc}\left(\frac{\sqrt{3}\lambda_3}{2\sigma}\right)\Bigg]. \end{aligned} \tag{15}$$

The above individual probability distributions, equations (13), (14), and (15), for the rescaled variable λ/σ are plotted in Figure 1. Note that the distribution of $\lambda_2(\boldsymbol{q})$ is Gaussian despite the fact that $\lambda_2(\boldsymbol{q})$ is not a Gaussian random field.

According to equation (15), $\lambda_3 > 0$ has a low probability of occurring, i.e., 0.08 (see Doroshkevich 1970 or Appendix A). However, the small value of $P(\lambda_3 > 0) = 0.08$ does not indicate that only 8% of all the regions will collapse into clumps. Rather, it indicates that the probability of finding a bound region at filtering mass scale M is 0.08, provided that it is included

[2] Doroshkevich (1970) derived the probability distribution of λ_1. But we found a typo in his result. Except for the typo, equation (13) agrees with his result.

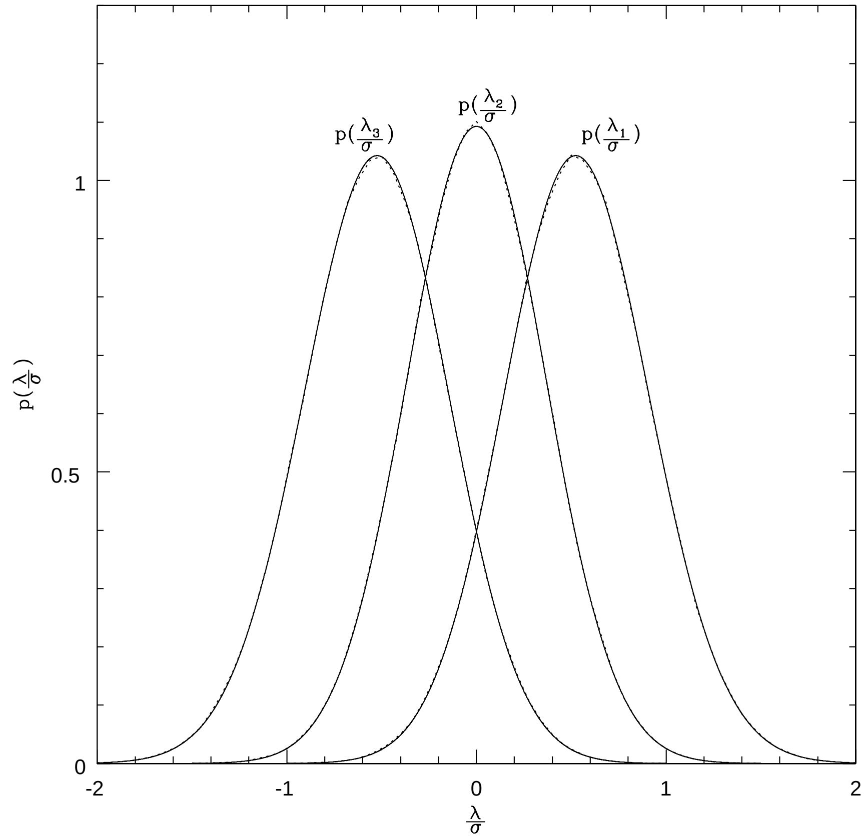

FIG. 1.—Individual probability distributions of three eigenvalues of the deformation tensor. The solid lines show the analytic results obtained in this paper for the rescaled variable λ/σ. The numerical results from the Monte Carlo simulation are also plotted (*dotted lines*).

in an isolated bound object with larger mass $M' > M$ (see § 5). Here the isolated bound objects indicate the bound objects that have just collapsed at a given epoch.

In the following subsection, we derive the conditional probabilities of $\lambda_3 > 0$ and δ, reveal the correlated properties between them, and determine a nonspherical collapse probability C.

3.2. *Conditional Probabilities*

In the linear regime when $D_+(t)$ is still less than unity, equation (10) can be approximated by

$$\rho \simeq \bar{\rho}[1 + D_+(\lambda_1 + \lambda_2 + \lambda_3)] . \tag{16}$$

Setting $D_+ \equiv 1$ at the present epoch, the linearly extrapolated density contrast is now written as

$$\delta = \frac{\delta\rho}{\bar{\rho}} = \lambda_1 + \lambda_2 + \lambda_3 . \tag{17}$$

Let us choose $(\delta, \lambda_2, \lambda_3)$ as a new set of variables. Then equation (12) can be reexpressed as a joint probability distribution of $(\delta, \lambda_2, \lambda_3)$ such that

$$p(\delta, \lambda_2, \lambda_3) = \frac{3375}{8\pi\sqrt{5}\sigma^6} \exp\left[-\frac{3\delta^2}{\sigma^2} + \frac{15}{2\sigma^2}(\lambda_2 + \lambda_3)(\delta - \lambda_2 - \lambda_3) + \frac{15}{2\sigma^2}\lambda_2\lambda_3\right](\delta - 2\lambda_2 - \lambda_3)(\lambda_2 - \lambda_3)(\delta - \lambda_2 - 2\lambda_3) . \tag{18}$$

Direct integration of the above joint distribution equation (18) over λ_2 gives the two-point probability distribution of (δ, λ_3):

$$\begin{aligned} p(\delta, \lambda_3) &= \int_{\lambda_3}^{(\delta-\lambda_3)/2} p(\delta, \lambda_2, \lambda_3) d\lambda_2 \\ &= \frac{3\sqrt{5}}{16\pi\sigma^4}(15\delta^2 - 90\lambda_3\delta + 135\lambda_3^2 - 8\sigma^2)\exp\left(-\frac{9\delta^2 - 30\lambda_3\delta + 45\lambda_3^2}{8\sigma^2}\right) + \frac{3\sqrt{5}}{2\sigma^2\pi}\exp\left(-\frac{6\delta^2 - 30\lambda_3\delta + 45\lambda_3^2}{2\sigma^2}\right), \end{aligned} \tag{19}$$

where the upper limit and the lower limit of λ_2 are $(\delta - \lambda_3)/2$ and λ_3, respectively, because of the condition of $\lambda_1 > \lambda_2 > \lambda_3$.

Using equation (19), we can investigate various correlated properties between the δ-field and the λ_3-field. First of all, let us calculate the probability distribution of δ confined in the regions with $\lambda_3 > 0$:

$$p(\delta \mid \lambda_3 > 0) = \frac{p(\delta, \lambda_3 > 0)}{P(\lambda_3 > 0)} = \frac{\int_0^{\delta/3} p(\delta, \lambda_3) d\lambda_3}{P(\lambda_3 > 0)}$$
$$= \left\{ -75\sqrt{5}/(8\pi\sigma^2)\delta \exp\left(-\frac{9\delta^2}{8\sigma^2}\right) + \frac{25}{4\sqrt{2\pi}\sigma} \exp\left(-\frac{\delta^2}{2\sigma^2}\right)\left[\operatorname{erf}\left(\frac{\delta\sqrt{10}}{4\sigma}\right) + \operatorname{erf}\left(\frac{\delta\sqrt{10}}{2\sigma}\right)\right]\right\} \Theta\delta \,. \tag{20}$$

Here Θ stands for the Heaviside step function and the condition $\lambda_1 > \lambda_2 > \lambda_3$ is used again to determine $\delta/3$ for the upper limit of λ_3. Figure 2 compares the unconditional Gaussian distribution of the density field equation (3) with this conditional probability distribution equation (20) for the rescaled variable δ/σ. It is shown that the maximum of $p(\delta \mid \lambda_3 > 0)$ is reached when $\delta \simeq 1.5\sigma$. That is, the linearly extrapolated density of the regions satisfying $\lambda_3 > 0$ is most likely to be around 1.5σ. The average density contrast, $\langle\delta\rangle_{\lambda_3 > 0}$, can be also computed with equation (20):

$$\langle\delta\rangle_{\lambda_3 > 0} = \int_0^\infty \delta p(\delta \mid \lambda_3 > 0) d\delta = \frac{25\sqrt{10}\sigma}{144\sqrt{\pi}} (3\sqrt{6} - 2) \simeq 1.65\sigma \,. \tag{21}$$

So, in the regions with $\lambda_3 > 0$, the average density $\langle\delta\rangle_{\lambda_3 > 0}$ is slightly higher than the most probable density, say, $\delta^{\max}_{\lambda_3 > 0}$. We note that for $\sigma = 1$, $\delta^{\max}_{\lambda_3 > 0}$ roughly coincides with the lowered density threshold $\delta_c \simeq 1.5$ of the PS mass function, while $\langle\delta\rangle_{\lambda_3 > 0}$ is close to the spherical threshold value $\delta_c \simeq 1.69$. Setting σ equal to 1 means filtering the density field on a characteristic mass scale M_* [defined by $\sigma(M_*) = 1$]. Thus the regions with $\lambda_3 > 0$ for $\sigma = 1$ correspond to clumps with masses $M > M_*$. In fact, as argued by Monaco (1995), it is unavoidable to limit our Lagrangian dynamical approach to the

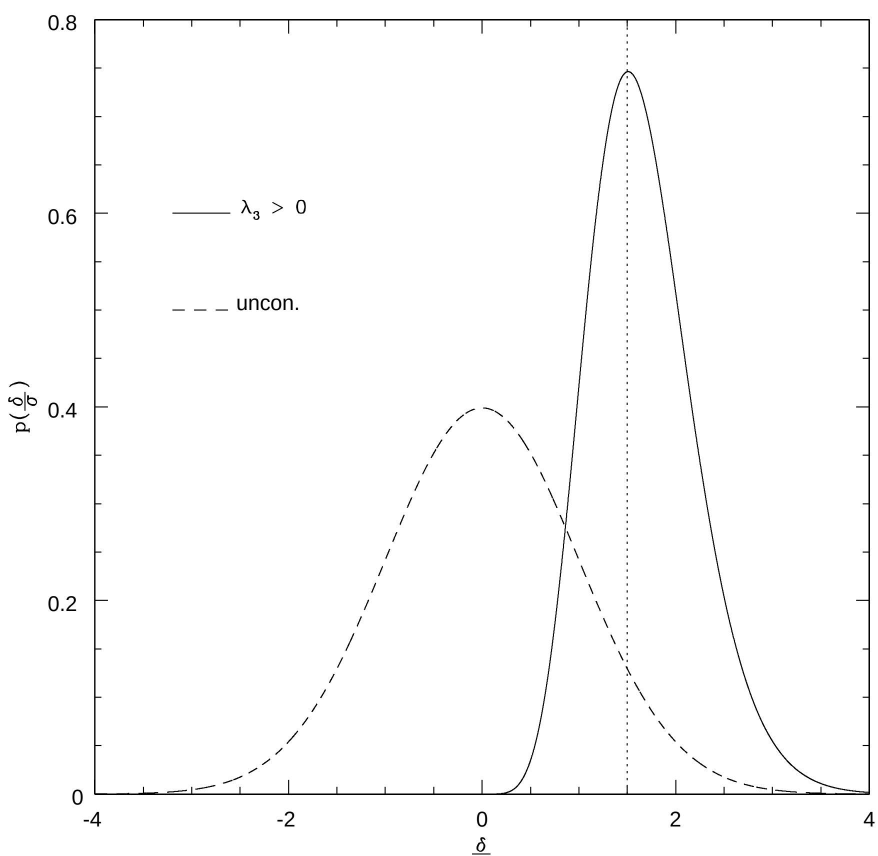

FIG. 2.—Probability distribution of the rescaled density field (δ/σ). The solid line represents the rescaled density distribution under the condition of $\lambda_3 > 0$, while the dashed line shows the unconditional Gaussian distribution. The vertical dotted line indicates the position of $\delta/\sigma = 1.5$.

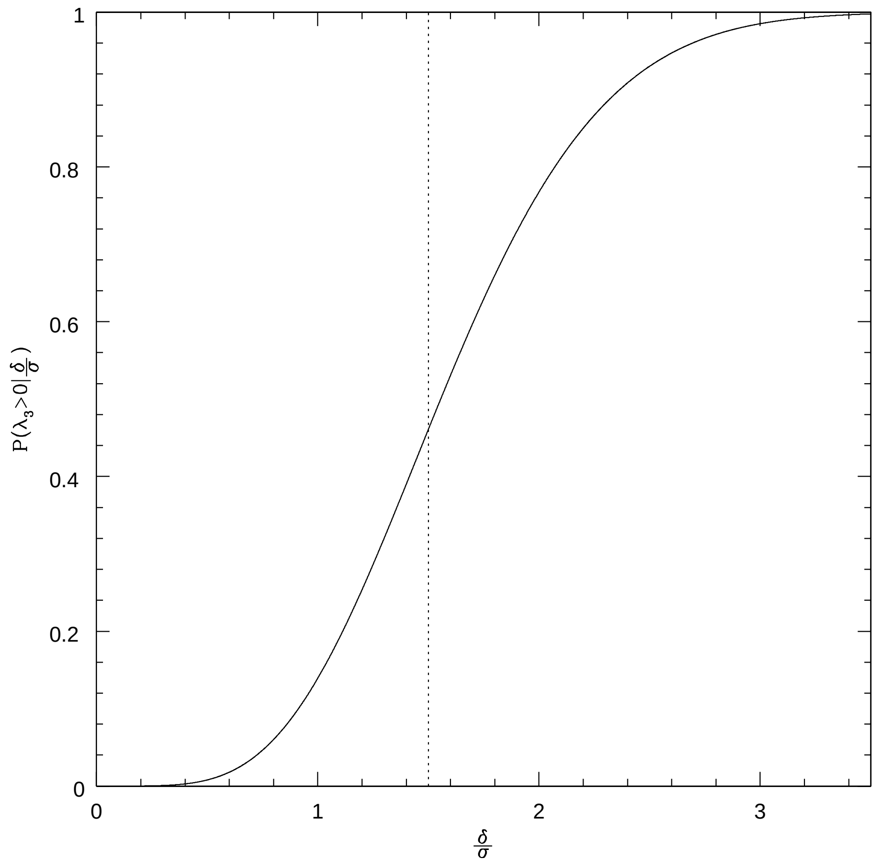

FIG. 3.—Conditional probability of $\lambda_3 > 0$ as a function of the rescaled density δ/σ. The vertical dotted line indicates the position $\delta/\sigma = 1.5$.

high-mass section ($M > M_*$) since the Zeldovich approximation is valid only in the single-stream regions, while the multistream regions are rare for $M > M_*$ (Kofman et al. 1994).

Another conditional distribution worth deriving is $P(\lambda_3 > 0 \,|\, \delta)$, the probability that a given region with density δ will have all positive eigenvalues:

$$\begin{aligned} P(\lambda_3 > 0 \,|\, \delta) &= \frac{p(\delta, \lambda_3 > 0)}{p(\delta)} \\ &= \left\{ -\frac{3\sqrt{10}}{4\sqrt{\pi}\sigma}\, \delta \exp\left(-\frac{5\delta^2}{8\sigma^2}\right) + \frac{1}{2}\left[\operatorname{erf}\left(\frac{\delta\sqrt{10}}{4\sigma}\right) + \operatorname{erf}\left(\frac{\delta\sqrt{10}}{2\sigma}\right)\right]\right\} \Theta\delta \,. \end{aligned} \tag{22}$$

The resulting conditional probability (22) for the rescaled variable δ/σ is plotted in Figure 3. The probability of $\lambda_3 > 0$ begins to exceed $\frac{1}{2}$ when $\delta \simeq 1.5\sigma$ and reaches unity when $\delta \simeq 3\sigma$. This implies that the collapse of highly overdense regions ($\delta \gg \sigma$) will be always along all three directions (see also Bernardeau 1994).

We take equation (22) as our nonspherical collapse probability C and proceed to derive the mass function of clumps analytically in the next section.

4. AN ANALYTIC APPROXIMATION TO MASS FUNCTIONS

As noted earlier, the Zeldovich approximation as a first-order Lagrangian theory works very well until the first orbit crossing (corresponding to the formation of pancakes) but breaks down afterward in the multistream regime (Shandarin & Zeldovich 1989). Therefore, the rather restrictive collapse condition based purely on this Lagrangian formalism may not be fully satisfactory to describe the formation of clumps, especially low-mass objects.

On the other hand, Shandarin & Klypin (1984) have shown by N-body simulations that the clumps form from the Lagrangian regions where the smallest eigenvalue λ_3 of the deformation tensor reaches a local maximum. Thus, one practical way to overcome the limited validity of the Zeldovich approximation within the framework of our dynamical approach to mass functions is to parameterize the collapse condition by $\lambda_3 > \lambda_{3c}$, assuming that the critical value of λ_{3c} is a free parameter. Employing this simple *Ansatz* to derive $n(M)$, we first calculate the following probability distribution with equations (3) and (19):

$$P(\lambda_3 > \lambda_{3c} \mid \delta) = \frac{p(\delta, \lambda_3 > \lambda_{3c})}{p(\delta)} = \frac{\int_{\lambda_{3c}}^{\delta/3} p(\delta, \lambda_3) d\lambda_3}{p(\delta)}$$
$$= \left(-\frac{3\sqrt{10}}{4\sqrt{\pi}\sigma}(\delta - 3\lambda_{3c})\exp\left[-\frac{5(\delta - 3\lambda_{3c})^2}{8\sigma^2}\right] + \frac{1}{2}\left\{\mathrm{erf}\left[\frac{(\delta - 3\lambda_{3c})\sqrt{10}}{4\sigma}\right] + \mathrm{erf}\left[\frac{(\delta - 3\lambda_{3c})\sqrt{10}}{2\sigma}\right]\right\}\right)\Theta(\delta - 3\lambda_{3c}) . \tag{23}$$

Comparison of equation (23) with equation (22) reveals that $P(\lambda_3 > \lambda_{3c} \mid \delta)$ is just horizontally shifted along the δ-axis by $3\lambda_{3c}$ from $P(\lambda_3 > 0 \mid \delta)$ with its shape unchanged.

Consequently, this *Ansatz* is mathematically equivalent to a parallel transformation of the density field itself by $-3\lambda_{3c}$. Thus, equation (1) is now expressed as follows:

$$F(M) = \int_{-1}^{\infty} p(\delta + 3\lambda_{3c}) \times P(\lambda_3 > 0 \mid \delta) d\delta ,$$
$$= \frac{1}{\sqrt{2\pi}\sigma}\int_0^{\infty} \exp\left[-\frac{(\delta + 3\lambda_{3c})^2}{2\sigma^2}\right]\left\{-\frac{75\sqrt{10}}{8\sqrt{\pi}\sigma}\,\delta \exp\left(-\frac{5\delta^2}{8\sigma^2}\right) + \frac{25}{4}\left[\mathrm{erf}\left(\frac{\delta\sqrt{10}}{4\sigma}\right) + \mathrm{erf}\left(\frac{\delta\sqrt{10}}{2\sigma}\right)\right]\right\} d\delta . \tag{24}$$

Here the volume fraction $F(M)$ is normalized by a factor of $1/0.08 = 12.5$, which we justify with a sharp k-space filter in § 5. This normalization factor is much larger than the factor of 2 in the PS formalism. However, this larger normalization factor can be explained by the larger amount of cloud-in-cloud occurrences in our dynamical formalism than in the PS formalism, as shown in § 5, where the amount of cloud-in-cloud occurrences is computed. In an ideal hierarchical model, all the masses are included in clumps. According to our dynamical model, only about 8% of all the masses are included in the clumps with the "largest" mass (the "largest" mass of bound objects in the universe is, in a practical sense, $M \simeq M_*$). This is in rough agreement with the fraction of the galaxies in the Abell clusters (e.g., Padmanabhan 1993). All the remaining masses are included in the clumps at smaller filtering mass scales.

Differentiating equation (24) with respect to σ, we have

$$\frac{\partial F}{\partial \sigma} = \frac{\partial}{\partial \sigma}\left(\frac{1}{\sqrt{2\pi}\sigma}\int_0^{\infty} \exp\left[-\frac{(\delta + 3\lambda_{3c})^2}{2\sigma^2}\right]\left\{-\frac{75\sqrt{10}}{8\sqrt{\pi}\sigma}\,\delta \exp\left(-\frac{5\delta^2}{8\sigma^2}\right) + \frac{25}{4}\left[\mathrm{erf}\left(\frac{\delta\sqrt{10}}{4\sigma}\right) + \mathrm{erf}\left(\frac{\delta\sqrt{10}}{2\sigma}\right)\right]\right\} d\delta\right)$$
$$= \frac{25\sqrt{10}\lambda_{3c}}{2\sqrt{\pi}\sigma^2}\left(\frac{5\lambda_{3c}^2}{3\sigma^2} - \frac{1}{12}\right)\exp\left(-\frac{5\lambda_{3c}^2}{2\sigma^2}\right)\mathrm{erfc}\left(\frac{\sqrt{2}\lambda_{3c}}{\sigma}\right) + \frac{25\sqrt{15}\lambda_{3c}}{8\sqrt{\pi}\sigma^2}\exp\left(-\frac{15\lambda_{3c}^2}{4\sigma^2}\right)\mathrm{erfc}\left(\frac{\sqrt{3}\lambda_{3c}}{2\sigma}\right)$$
$$- \frac{125\sqrt{5}\lambda_{3c}^2}{6\pi\sigma^3}\exp\left(-\frac{9\lambda_{3c}^2}{2\sigma^2}\right). \tag{25}$$

Figure 4 shows the generic behavior of this differential volume fraction (25) as λ_{3c} changes. Since $\partial F/\partial\sigma$ is directly proportional to $n(M)$, one can conclude from Figure 4 that as λ_{3c} increases, the number densities of small-mass clumps (large σ) increase while the large masses (small σ) are reduced and the peak is lowered.

For simple power-law spectra $|\delta_k|^2 \propto k^n$, the mass variance becomes

$$\sigma^2(M) = \left(\frac{M}{M_*}\right)^{-(n+3)/3} . \tag{26}$$

So in this case, the mass function can be expressed explicitly in terms of M:

$$n(M) = \frac{\bar{\rho}}{M}\left|\frac{dF}{dM}\right| = \frac{\bar{\rho}}{M}\left|\frac{d\sigma}{dM}\frac{\partial F}{\partial \sigma}\right|$$
$$= \frac{25\sqrt{10}\lambda_{3c}}{2\sqrt{\pi}}\left(\frac{n+3}{6}\right)\frac{\bar{\rho}}{M^2}\left(\frac{M}{M_*}\right)^{(n+3)/6}\left\{\left[\frac{5\lambda_{3c}^2}{3}\left(\frac{M}{M_*}\right)^{(n+3)/3} - \frac{1}{12}\right]\exp\left[-\frac{5\lambda_{3c}^2}{2}\left(\frac{M}{M_*}\right)^{(n+3)/3}\right]\right.$$
$$\times\,\mathrm{erfc}\left[\sqrt{2}\lambda_{3c}\left(\frac{M}{M_*}\right)^{(n+3)/6}\right] + \frac{\sqrt{6}}{8}\exp\left[-\frac{15\lambda_{3c}^2}{4}\left(\frac{M}{M_*}\right)^{(n+3)/3}\right]\mathrm{erfc}\left[\frac{\sqrt{3}\lambda_{3c}}{2}\left(\frac{M}{M_*}\right)^{(n+3)/6}\right]$$
$$\left. - \frac{5\lambda_{3c}}{3\sqrt{2\pi}}\left(\frac{M}{M_*}\right)^{(n+3)/6}\exp\left[-\frac{9\lambda_{3c}^2}{2}\left(\frac{M}{M_*}\right)^{(n+3)/3}\right]\right\} . \tag{27}$$

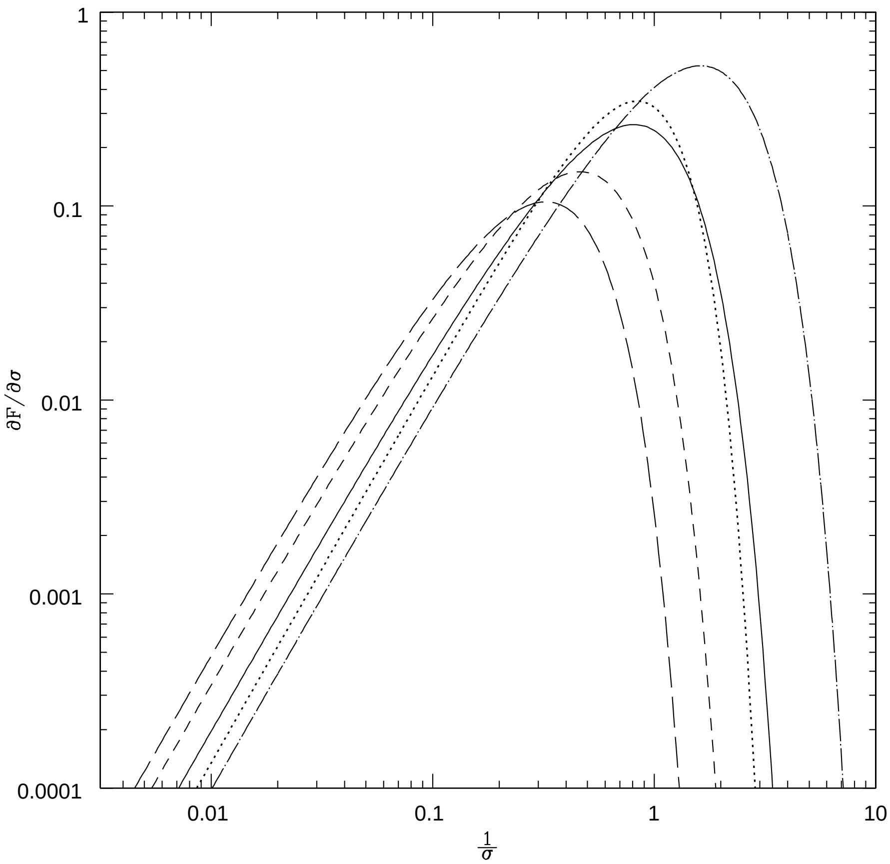

FIG. 4.—Differential volume fraction for $\lambda_{3c} = 0.1$, 0.4, 0.7, and 1.0 (*dot-dashed, solid, dashed, and long-dashed lines*). The dotted line is the standard ($\delta_c \simeq 1.69$) PS differential volume fraction.

We display the resulting mass function for $\lambda_{3c} \simeq 0.37$ in Figure 5. The value of 0.37 for λ_{3c} is chosen to make our results for the high-mass section fit well with the $\delta_c \simeq 1.5$ PS mass function, which has been tested to be a good approximation (see Monaco 1995). The original PS mass function with $\delta_c \simeq 1.69$ is also shown for comparison. For every power index n from -2 to 1, the mass function equation (27) is characterized by the following properties:

1. In the high-mass section ($M/M_* > 1$), it fits quite well with the $\delta_c \simeq 1.5$ PS mass function.
2. Its peak is lower than that of the PS one, which agrees with N-body results (see, e.g., Efstathiou et al. 1988).
3. It has approximately the same slope as the PS mass function but predicts more structures in the low-mass section ($M/M_* < 1$).

5. NORMALIZATION

Up to now, following the PS-like approach, we assumed that equation (2) is correct. In other words, the probability of finding a region with $\lambda_3 > \lambda_{3c}$ at a filtering mass scale M is assumed to be proportional to the fraction of the volume occupied by the regions that will eventually collapse into bound objects with masses greater than or equal to M.

Strictly speaking, however, equation (2) is not quite correct since the resulting mass function always has to be renormalized. Even in the regions with $\lambda_3 < \lambda_{3c}$ at the filtering mass scale M, there is still a nonzero probability of $\lambda_3 = \lambda_{3c}$ when the density field is filtered at some larger scale $M'(>M)$. But this marginal probability is ignored by the PS-like approach, which has resulted in a large normalization factor 12.5 of our mass function.

Jedamzik (1995) suggested a generalization of equation (2):[3]

$$\left|\frac{dF}{dM}\right| = \frac{d}{dM}\left|\int_0^\infty dM' n(M') \frac{M'}{\bar{\rho}} P(M, M')\right| . \tag{28}$$

Here $P(M, M')$ is the conditional probability of finding a bound region ($\lambda_3 > \lambda_{3c}$) at filtering mass scale M, provided that it is included in an isolated bound object ($\lambda_3 = \lambda_{3c}$) with mass $M'(>M)$. The isolated bound objects at a given epoch are those that have just collapsed. Thus, in our formalism, the isolated bound objects correspond to the regions with $\lambda_3 = \lambda_{3c}$ at a given filtering mass scale.

[3] In the original analysis based on the top-hat spherical model, Jedamzik (1995) did not use a mathematically correct definition of isolated bound objects.

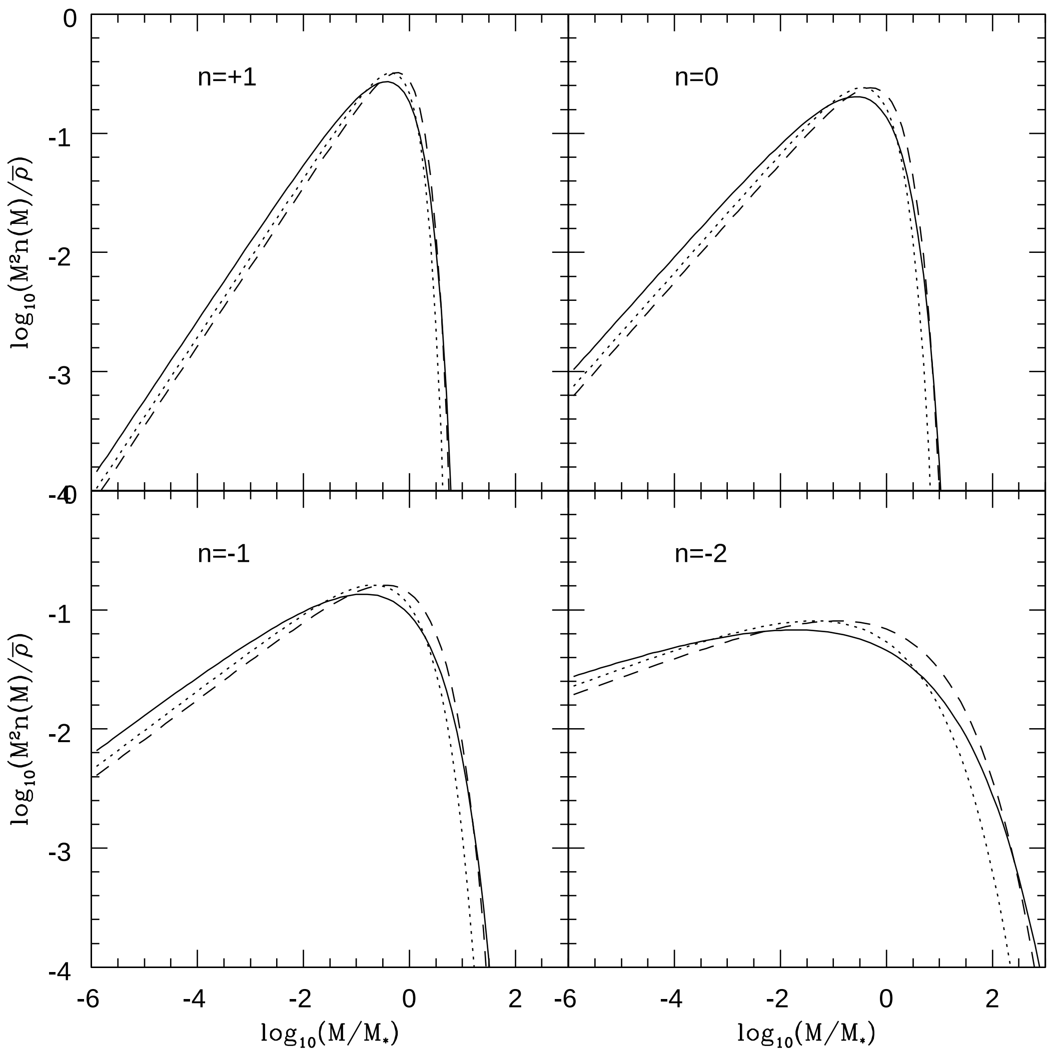

FIG. 5.—Mass function for the power index $n = +1, 0, -1$, and -2. The solid lines show our analytic results with $\lambda_{3c} = 0.37$, while the dashed and dotted lines represent the PS mass function with $\delta_c = 1.5$ and 1.69, respectively.

We find that the conditional probability $P(M, M')$ for the case of a sharp k-space filter is given by (see Appendix B)

$$P(M, M') = 0.08\Theta(M' - M) . \tag{29}$$

Equation (29) reveals that $P(\lambda_3 > 0) = 0.08$ results in $P(M, M') = 0.08$ $(M < M')$. So, in our formalism, the probability of finding a bound region ($\lambda_3 > \lambda_{3c}$) of mass scale M included in an isolated bound region ($\lambda_3 = \lambda_{3c}$) with mass greater M is only 0.08. And this is directly related to our normalization factor of $1/0.08 = 12.5$. Whereas in the PS formalism, the probability $P(M, M')$ is 0.5, which is again directly related to the PS normalization factor of $1/0.5 = 2$.

Now, with equations (28) and (29), we have

$$\left|\frac{dF}{dM}\right| = 0.08 \int_0^\infty dM' n(M') \frac{M'}{\bar{\rho}} \delta_{\rm D}(M' - M)$$
$$= 0.08 \frac{M}{\bar{\rho}} n(M) , \tag{30}$$

where $\delta_{\rm D}$ stands for the Dirac delta function. More explicitly,

$$n(M) = 12.5 \frac{\bar{\rho}}{M}\left|\frac{dF}{dM}\right| , \tag{31}$$

which is exactly the same formula as equation (2) with the normalization factor of 12.5 explicitly included.

Thus equation (31) justifies the normalization factor 12.5 of our mass function in the case of a sharp k-space filter.

6. DISCUSSION AND CONCLUSIONS

We have derived an *analytic* approximation of the mass distribution function for clumps. The underlying dynamics has been described by the Zeldovich approximation, which treats the nonspherical gravitational collapse. Like Shandarin &

Klypin (1984) and Audit et al. (1997), we have assumed that the clumps would be formed by the mass elements that have experienced gravitational collapse along all three directions.

We have given a somewhat different interpretation to the PS analysis by reexpressing the fraction of the volume occupied by the bound regions in terms of two probabilities: the probability of the Gaussian density distribution and the collapse probability of the given dense regions. The Zeldovich approximation has led us to determine a nonspherical collapse probability that is different from the PS one, relating the density field to the positive lowest eigenvalue of the deformation tensor.

We have shown that the collapse probability reaches almost unity when $\delta > 3\sigma$, which indicates that the highly overdense regions will always collapse along all three directions. In addition, we have found the density distribution of the regions that meet the collapse condition based on the Zeldovich approximation. This distribution has shown that the most probable density contrast of such regions is around 1.5 at the characteristic mass scale M_*.

We have proposed a simple *Ansatz* in order to treat the multistream regions where the Lagrangian dynamics is not applicable. This *Ansatz* has enabled us to derive an analytic mass function characterized by one free parameter, λ_{3c}. The best approximate value of this parameter was chosen to be $\lambda_{3c} \simeq 0.37$. We admit that there is no background dynamical theory for determining directly the value of this free parameter, which thus has to be found phenomenologically. However, the following arguments may give a clue to understanding why this parameter has this value. A simple extrapolation of equation (10) into the multistream regions suggests that only the mass elements with $\lambda_3 > \lambda_{3c} = 1$ collapse along all three directions by the present epoch of $D_+ = 1$. However, the collapse along the first two directions increases the density, which therefore speeds up the collapse along the third direction. This roughly agrees with the conclusion of Audit et al. (1997). Using equation (24) from Audit et al. (1997) with their choice of the parameters ($\epsilon = 1$, $\alpha = 0.8$, $\delta_c = 1.69$, $\sigma_c = 0.74$), one can easily obtain for the collapse epoch $a_c = 1/(0.8\lambda_3 + 0.32\delta)$, which is always earlier than the prediction of the Zeldovich approximation ($a_c = 1/\lambda_3$), provided that $\lambda_3 > 0$.

For power-law spectra, it has been shown that our resulting mass function with $\lambda_{3c} \simeq 0.37$ is in good agreement with the $\delta_c \simeq 1.5$ PS mass function in the high-mass section but has a lower peak and predicts more small-mass structures, which are in agreement with what has been detected in N-body simulations (e.g., Efstathiou et al. 1988; Peacock & Heavens 1990). However, it should be noted that the prediction concerning the small-mass structures is least reliable not only in any PS-like approach but also in our dynamical approach to the mass function since the validity domain of the Zeldovich approximation is limited to the high-mass section as outlined in § 3.2.

Like the other PS-like formalisms, a normalization factor for the mass function has been introduced, which in our case is 12.5. We have justified the normalization factor with a sharp k-space filter by using the Jedamzik integral equation, showing that this rather large normalization factor is due to the low probability of finding a bound region ($\lambda_3 > \lambda_{3c}$) at filtering mass scale M included in an isolated bound region ($\lambda_3 = \lambda_{3c}$) with larger mass M'. But the physical meaning of the sharp k-space filter has yet to be fully understood.

We postpone the numerical testing of our mass function to a later paper.

We are grateful to Lev Kofman, Paolo Catelan, and the referee for useful discussions and helpful comments. This work has been done under the support of NASA grant NAG 5-4039 and an EPSCoR 1996 grant.

APPENDIX A

In 1970, Doroshkevich found the joint probability distribution, $p(\lambda_1, \lambda_2, \lambda_3)$, of an ordered set of eigenvalues (eq. [12] in § 3.1), corresponding to a Gaussian potential. In this Appendix, we sketch the derivation of $p(\lambda_1)$, $p(\lambda_2)$, and $p(\lambda_3)$ (eqs. [13], [14], and [15] in § 3.1) and investigate their statistical properties.

The two-point probability distributions, $p(\lambda_1, \lambda_2)$, $p(\lambda_2, \lambda_3)$, and $p(\lambda_1, \lambda_3)$ can be easily obtained from the direct integration of $p(\lambda_1, \lambda_2, \lambda_3)$ such that

$$\begin{aligned} p(\lambda_1, \lambda_2) &= \int_{-\infty}^{\lambda_2} p(\lambda_1, \lambda_2, \lambda_3) d\lambda_3 \\ &= \frac{1125}{64\sqrt{5}\pi\sigma^4} \left\{ (\lambda_1 - \lambda_2)(3\lambda_1 - \lambda_2) \exp\left(-\frac{3\lambda_1^2}{\sigma^2} + \frac{3\lambda_1\lambda_2}{\sigma^2} - \frac{9\lambda_2^2}{2\sigma^2} \right) \right. \\ &\quad + \frac{\sqrt{3\pi}\sigma}{12} (\lambda_1 - \lambda_2) \left[8 + \frac{3}{\sigma^2} (3\lambda_1 - \lambda_2)(3\lambda_2 - \lambda_1) \right] \\ &\quad \left. \times \exp\left(-\frac{45\lambda_1^2}{16\sigma^2} + \frac{15\lambda_1\lambda_2}{8\sigma^2} - \frac{45\lambda_2^2}{16\sigma^2} \right) \operatorname{erfc}\left[\frac{\sqrt{3}}{4\sigma} (\lambda_1 - 3\lambda_2) \right] \right\} \Theta(\lambda_1 - \lambda_2) , \end{aligned} \tag{A1}$$

$$\begin{aligned} p(\lambda_2, \lambda_3) &= \int_{\lambda_2}^{\infty} p(\lambda_1, \lambda_2, \lambda_3) d\lambda_1 \\ &= \frac{1125}{64\sqrt{5}\pi\sigma^4} \left\{ (\lambda_2 - \lambda_3)(\lambda_2 - 3\lambda_3) \exp\left(-\frac{3\lambda_3^2}{\sigma^2} + \frac{3\lambda_2\lambda_3}{\sigma^2} - \frac{9\lambda_2^2}{2\sigma^2} \right) \right. \end{aligned}$$

$$+\frac{\sqrt{3\pi}\sigma}{12}(\lambda_2-\lambda_3)\left[8+\frac{3}{\sigma^2}(\lambda_2-3\lambda_3)(\lambda_3-3\lambda_2)\right]$$
$$\times\exp\left(-\frac{45\lambda_2^2}{16\sigma^2}+\frac{15\lambda_2\lambda_3}{8\sigma^2}-\frac{45\lambda_3^2}{16\sigma^2}\right)\mathrm{erfc}\left[\frac{\sqrt{3}}{4\sigma}(3\lambda_2-\lambda_3)\right]\Bigg\}\Theta(\lambda_2-\lambda_3)\,, \tag{A2}$$

$$p(\lambda_1,\lambda_3)=\int_{\lambda_3}^{\lambda_1}p(\lambda_1,\lambda_2,\lambda_3)d\lambda_2$$
$$=\frac{1125}{64\sqrt{5\pi}\sigma^4}\Bigg((\lambda_1-\lambda_3)(3\lambda_1-\lambda_3)\exp\left(-\frac{3\lambda_1^2}{\sigma^2}+\frac{3\lambda_1\lambda_3}{\sigma^2}-\frac{9\lambda_3^2}{2\sigma^2}\right)$$
$$+(\lambda_1-\lambda_3)(\lambda_1-3\lambda_3)\exp\left(-\frac{3\lambda_3^2}{\sigma^2}+\frac{3\lambda_1\lambda_3}{\sigma^2}-\frac{9\lambda_1^2}{2\sigma^2}\right)$$
$$+\frac{\sqrt{3\pi}\sigma}{12}(\lambda_1-\lambda_3)\left[\frac{3}{\sigma^2}(3\lambda_1-\lambda_3)(\lambda_1-3\lambda_3)-8\right]\times\exp\left(-\frac{45\lambda_1^2}{16\sigma^2}+\frac{15\lambda_1\lambda_3}{8\sigma^2}-\frac{45\lambda_3^2}{16\sigma^2}\right)$$
$$\times\left\{\mathrm{erfc}\left[\frac{\sqrt{3}}{4\sigma}(3\lambda_1-\lambda_3)\right]-\mathrm{erfc}\left[\frac{\sqrt{3}}{4\sigma}(3\lambda_3-\lambda_1)\right]\right\}\Bigg)\Theta(\lambda_1-\lambda_3) \tag{A3}$$

In order to derive $p(\lambda_1)$, $p(\lambda_2)$, and $p(\lambda_3)$, we have to integrate the above two-point distributions, which involve complex error function terms as one can see. We find the following recursion formula, which is useful in integrating such complex terms:

$$\int t^n\exp(-a^2t^2)\mathrm{erf}(bt)dt=\frac{n-1}{2a^2}\int t^{n-2}\exp(-a^2t^2)\,\mathrm{erf}(bt)dt$$
$$-\frac{1}{2a^2}t^{n-1}\exp(-a^2t^2)\,\mathrm{erf}(bt)+\frac{b}{a^2\sqrt{\pi}}\int t^{n-1}\exp[-(a^2+b^2)t^2]dt\,. \tag{A4}$$

With the above recursion formula, it is straightforward to derive the individual distributions. The results are shown in § 3.1 (eqs. [13], [14], and [15]).

Now the probability that each eigenvalue is positive as well as the mean and the variance of each eigenvalue can be computed with the above results:

$$P(\lambda_1>0)=23/25\,,\qquad P(\lambda_2>0)=\tfrac{1}{2}\,,\qquad P(\lambda_3>0)=2/25\,; \tag{A5}$$

$$\bar{\lambda}_1=\frac{3}{\sqrt{10\pi}}\sigma\,,\qquad \bar{\lambda}_2=0\,,\qquad \bar{\lambda}_3=-\frac{3}{\sqrt{10\pi}}\sigma\,; \tag{A6}$$

$$\sigma_{\lambda_1}^2=\frac{13\pi-27}{30\pi}\sigma^2\,,\qquad \sigma_{\lambda_2}^2=\frac{2}{15}\sigma^2\,,\qquad \sigma_{\lambda_3}^2=\frac{13\pi-27}{30\pi}\sigma^2\,; \tag{A7}$$

which are all in agreement with Doroshkevich (1970).

APPENDIX B

In the framework of our formalism, the conditional probability $P(M, M')$ is written as

$$P(M,M')=P(\lambda_3>\lambda_{3c}\,|\,\lambda_3'=\lambda_{3c})=\frac{P(\lambda_3>\lambda_{3c},\lambda_3'=\lambda_{3c})}{P(\lambda_3'=\lambda_{3c})}\,, \tag{B1}$$

where λ_3 and λ_3' are the lowest eigenvalues of the deformation tensor at the same point but at two different filtering mass scales, M and M', respectively.

In order to derive the probability $P(\lambda_3>\lambda_{3c}, \lambda_3'=\lambda_{3c})$, we start with the multivariate Gaussian joint probability distribution (see Doroshkevich 1970; Bardeen et al. 1986) for the six independent elements of the deformation tensor at two different mass scales:

$$p_J(y_1,\ldots,y_6')dy_1,\ldots,dy_6'=\frac{\exp(-Q)}{(2\pi)^6\sqrt{\det(V)}}dy_1,\ldots,dy_6'\,, \tag{B2}$$

$$Q=\tfrac{1}{2}\boldsymbol{y}^t\cdot\boldsymbol{V}\cdot\boldsymbol{y}\,. \tag{B3}$$

Here V is the covariance matrix, while $\{y_i\}_{i=1}^6$ and $\{y_1'\}_{i=1}^6$ are the six independent elements of the deformation tensor (defined by eq. [11] in § 3.1; $y_1\equiv d_{11}$, $y_2\equiv d_{22}$, $y_3\equiv d_{33}$, $y_4\equiv d_{12}$, $y_5\equiv d_{23}$, $y_6\equiv d_{31}$) at mass scales M and M', respectively.

In the case of a sharp k-space filter, the mutual correlations between $\{y_i\}_{i=1}^6$ and $\{y'_1\}_{i=1}^6$ are

$$\langle y_i^2 \rangle = \frac{\sigma_M^2}{5}, \qquad \langle y_i y_j \rangle = \frac{\sigma_M^2}{15}, \qquad \langle y_i y'_i \rangle = \frac{\sigma_{M'}^2}{5}, \tag{B4}$$

$$\langle y_i'^2 \rangle = \frac{\sigma_{M'}^2}{5}, \qquad \langle y'_i y'_j \rangle = \frac{\sigma_{M'}^2}{15}, \qquad \langle y_i y'_j \rangle = \frac{\sigma_{M'}^2}{15}, \tag{B5}$$

for $i, j(\neq i) = 1, 2, 3$, and

$$\langle y_i^2 \rangle = \frac{\sigma_M^2}{15}, \qquad \langle y_i y_j \rangle = 0, \qquad \langle y_i y'_i \rangle = \frac{\sigma_{M'}^2}{15}, \tag{B6}$$

$$\langle y_i'^2 \rangle = \frac{\sigma_{M'}^2}{15}, \qquad \langle y'_i y'_j \rangle = 0, \qquad \langle y_i y'_j \rangle = 0, \tag{B7}$$

for $i, j(\neq i) = 4, 5, 6$. Here σ_M^2 and $\sigma_{M'}^2$ are the mass variance of the density field filtered at the mass scales M and M', respectively.

From equations (B2)–(B7), along with the similarity transformation of the deformation tensor into its principal axes, we find the following joint probability distribution of the three eigenvalues $\{\lambda_i\}_{i=1}^3$, $\{\lambda'_i\}_{i=1}^3$ of the deformation tensor at filtering mass scales M, $M'(M < M')$, respectively:

$$p_J(\lambda_1, \ldots, \lambda'_3) d\lambda_1, \ldots, d\lambda'_3 = p_{J1}(\Delta_1, \Delta_2, \Delta_3) d\Delta_1\, d\Delta_2\, d\Delta_3 \times p_{J2}(\lambda'_1, \lambda'_2, \lambda'_3) d\lambda'_1\, d\lambda'_2\, d\lambda'_3, \tag{B8}$$

$$p_{J1} = \frac{5^3 \times 3^3}{2^4 \pi^3 \sigma_\Delta^6 \sqrt{5}} \exp\left(-\frac{3I_1^2}{\sigma_\Delta^2} + \frac{15 I_2}{2\sigma_\Delta^2}\right)(\Delta_1 - \Delta_2)(\Delta_2 - \Delta_3)(\Delta_3 - \Delta_1), \tag{B9}$$

$$p_{J2} = \frac{5^3 \times 3^3}{2^4 \pi^3 \sigma_{M'}^6 \sqrt{5}} \exp\left(-\frac{3I_1'^2}{\sigma_{M'}^2} + \frac{15 I'_2}{2\sigma_{M'}^2}\right)(\lambda'_1 - \lambda'_2)(\lambda'_2 - \lambda'_3)(\lambda'_3 - \lambda'_1), \tag{B10}$$

where

$$\Delta_i \equiv \lambda_i - \lambda'_i, \qquad \sigma_\Delta^2 \equiv \sigma_M^2 - \sigma_{M'}, \tag{B11}$$

$$I_1 \equiv \Delta_1 + \Delta_2 + \Delta_3, \qquad I_2 \equiv \Delta_1 \Delta_2 + \Delta_2 \Delta_3 + \Delta_3 \Delta_1, \tag{B12}$$

$$I'_1 \equiv \lambda'_1 + \lambda'_2 + \lambda'_3, \qquad I'_2 \equiv \lambda'_1 \lambda'_2 + \lambda'_2 \lambda'_3 + \lambda'_3 \lambda'_1. \tag{B13}$$

Note the similarity between p_{J1} and p_{J2}. In fact, the above equations are useful only in the case of a sharp k-space filter.

The integration of p_J over λ_1, λ_2, λ'_1, and λ'_2 gives us the joint probability density distribution, $p(\lambda_3, \lambda'_3)$:

$$p(\lambda_3, \lambda'_3) d\lambda_3\, d\lambda'_3 = p(\Delta_3) d\Delta_3\, p(\lambda'_3) d\lambda'_3. \tag{B14}$$

Here the probability density distributions of $p(\Delta_3)$ and $p(\lambda'_3)$ have the same form as $p(\lambda_3)$ (eq. [15]) except for the value of the variance.

Finally, we derive the conditional probability $P(M, M')$:

$$\begin{aligned} P(M, M') &= \frac{P(\lambda_3 > \lambda_{3c}, \lambda'_3 = \lambda_{3c})}{P(\lambda'_3 = \lambda_{3c})} = \frac{p(\lambda'_3 = \lambda_{3c}) d\lambda'_3 \int_0^\infty d\Delta_{3c}\, p(\Delta_{3c})}{p(\lambda'_3 = \lambda_{3c}) d\lambda'_3} \\ &= \int_0^\infty d\Delta_{3c}\, p(\Delta_{3c}) = \int_0^\infty d\lambda_3\, p(\lambda_3) = 0.08\Theta(M' - M), \end{aligned} \tag{B15}$$

where Δ_{3c} is $\lambda_3 - \lambda_{3c}$.

REFERENCES

Arnold, V. I., Shandarin, S. F., & Zeldovich, Ya. B. 1982, Geophys. Astrophys. Fluid Dyn., 20, 111
Audit, E., Teyssier, R., & Alimi, J. M. 1997, A&A, 325, 439
Bardeen, J. M., Bond, J. R., Kaiser, N., & Szalay, A. S. 1986, ApJ, 304, 15
Bernardeau, F. 1994, ApJ, 427, 51
Bond, J. R., Cole, S., Efstathiou, G., & Kaiser, N. 1991, ApJ, 379, 440
Bond, J. R., & Myers, S. T. 1996, ApJS, 103, 1
Brainerd, T. G., & Villumsen, J. V. 1992, ApJ, 394, 409
Carlberg, R. G., & Couchman, H. M. P. 1989, ApJ, 340, 47
Cavaliere, A., & Menci, N. 1993, ApJ, 407, L9
———. 1994, ApJ, 435, 528
Cavaliere, A., Menci, N., & Tozzi, P. 1996, ApJ, 464, 44
Doroshkevich, A. G. 1967, Astrofizika, 3, 175
———. 1970, Astrofizika, 6, 581
Efstathiou, G., Frenk, C. S., White, S. D. M., & Davis, M. 1988, MNRAS, 235, 715
Efstathiou, G., & Rees, M. J. 1988, MNRAS, 230, 5
Jedamzik, K. 1995, ApJ, 448, 1
Klypin, A., Borgani, S., Holtzman, J., & Primack, J. 1995, ApJ, 444, 1
Kofman, L., Bertschinger, E., Gelb, J. M., Nusser, A., & Dekel, A. 1994, ApJ, 420, 44
Kolb, E. W., & Turner, M. S. 1990, The Early Universe (New York: Addison-Wesley)
Kuhlman, B., Melott, A. L., & Shandarin, S. F. 1996, ApJ, 470, L41
Lacey, C. & Cole, S. 1994, MNRAS, 271, 676
Lucchin, F. 1988, in Morphological Cosmology, ed. P. Flin & H. W. Duerbeck (Berlin: Springer), 284
Monaco, P. 1995, ApJ, 447, 23
———. 1997, preprint (astro-ph/9710085)
Padmanabhan, T. 1993, Structure Formation in the Universe (Cambridge: Cambridge Univ. Press)
Peacock, J. A., & Heavens, A. F. 1990, MNRAS, 243, 133
Peebles, P. J. E. 1985, ApJ, 297, 350
———. 1990, ApJ, 365, 27
———. 1993, Principles of Physical Cosmology (Princeton: Princeton Univ. Press)

Press, W. H., & Schechter, P. 1974, ApJ, 187, 425 (PS)
Shandarin, S. F., & Klypin, A. A. 1984, Soviet Astron., 28, 491
Shandarin, S. F., Melott, A. L., McDavitt, K., Pauls, J. L., & Tinker, J. 1995, Phys. Rev. Lett., 75, 7
Shandarin, S. F., & Zeldovich, Ya. B. 1989, Rev. Mod. Phys., 61, 185
Silk, J., & White, S. D. 1978, ApJ, 223, L59
Vergassola, M., Dubrulle, B., Frisch, U., & Noullez, A. 1994, A&A, 289, 325
Williams, B. G., Heavens, A. F., Peacock, J. A., & Shandarin, S. F. 1991, MNRAS, 250, 458
Yano, T., Nagashima, M., & Gouda, N. 1996, ApJ, 466, 1
Zeldovich, Ya. B. 1970, A&A, 5, 84